Ablation and Thermal Depths in VSP Er:YAG Laser Skin Resurfacing

Matjaz Lukac[1], Tadej Perhavec[2], Karolj Nemes[2], Uros Ahcan[3]
[1]Institut Josef Stefan, Department for Complex Matter, Jamova 39, Ljubljana, Slovenia
[2]Fotona d.d., Ljubljana, Slovenia
[3]Cinical Center Ljubljana, Department of Plastic Surgery and Burns, Ljubljana, Slovenia

ABSTRACT:

The list of indications for which Variable Square Pulse (VSP) Er:YAG laser systems can be used is continuously expanding. For example, ablative fractional resurfacing treatments performed with the VSP Er:YAG laser have good clinical outcomes and significantly shorter recovery times and adverse effects compared with traditional ablative laser skin resurfacing. Recently, an Er:YAG laser operating in variable pulse length, non-ablative, SMOOTH mode, for use in new collagen synthesis, has been introduced. The broad range of available Er:YAG modes of operation call for a more systematic understanding of the thermal and ablative effects this laser has on skin tissue. In this study, a theoretical micro-explosions computer (MEC) model is developed that explicitly links laser and tissue parameters with the clinical end effects of ablation and residual heat deposition. The computed results are then compared with experimental measurements of ablation rates and heat deposition in skin. The MEC model is found to be in good agreement with experiment, and has already been implemented in the latest VSP Er:YAG laser systems as a software tool for automatic calculation of the expected ablation and thermal depths in clinical procedures.

Key words: Er:YAG laser; Variable Square Pulse; VSP technology; ablation depth; thermal depth; fractional; laser resurfacing; SMOOTH mode; TURBO mode;

Article: J. LAHA, Vol. 2010, No. 1, pp- 56-71.
Received: March 03, 2010; Accepted: March 30, 2010.

© *Laser and Health Academy. All rights reserved.*
Printed in Europe. www.laserandhealth.com

I. INTRODUCTION

In the last decade, cutaneous laser resurfacing has gained popularity among laser surgeons and the public. [1] Removing the outer skin layers to the papillary dermis level induces re-epithelialisation and new collagen formation, which can create a smoother, even-toned, and more youthful appearance. Lasers currently available for cutaneous resurfacing include high-energy pulsed or scanned carbon dioxide lasers, short-pulsed Er:YAG or Er:YSGG lasers, [2-5] and Variable Square Pulse (VSP) Er:YAG laser systems.[6] Carbon dioxide laser skin resurfacing can achieve excellent clinical improvement of photodamage, rhytides, and atrophic scars. However, this resurfacing is associated with an extended reepithelialization period and, in some cases, prolonged erythema that may persist for several months. Of greater concern is the potential for delayed permanent hypopigmentation seen in as many as 20% of patients when multiple-pass carbon dioxide resurfacing is performed. The demand for less aggressive modalities for skin rejuvenation led to the development of the Er:YAG laser. [1,2]

The cutaneous absorption of the Er:YAG laser energy by water is 10-times more efficient then the absorption of carbon dioxide laser, allowing for more superficial tissue ablation and finer control. Because of these advantages, the pulsed Er:YAG laser superseded the carbon dioxide laser as a superlative ablative modality. In addition, the latest Variable Square Pulse (VSP) technology Er:YAG lasers have variable pulse widths and pulse sequences, allowing the practitioner to select the effect of the laser from "cold" ablation peeling to deeper thermal thermal. [7-9] Indications include mildly photo-damaged skin lesions (e.g. solar keratoses), mildly atrophic facial scars (e.g. from acne or varicella), dyschromias (e.g. melasma, lentigines), and mild-to-moderate facial wrinkles in the perioral, periocular, and cheek areas.[10-13] Newer Er:YAG lasers with longer and variable pulses allow patients with deeper wrinkles and scars to be successfully treated. In addition, Scanner Optimized Efficacy (SOE) [14] technology eliminates the need for manually aiming a small to medium spot size laser beam hundreds of times to cover a large skin area. SOE utilizes computer-controlled scanner mirrors to automatically place a laser beam in a perfect nonsequential or controlled random pattern.

Many other skin lesions have been successfully treated with the VSP Er:YAG laser, including compound nevi, sebaceous hyperplasia, trichoepitheliomas, miliary osteomas, syringoma, telangiectasia, rhinophyma, adenoma sebaceum, hidradenoma, xanthelasma, and the cutaneous manifestations of Hailey-Hailey disease and Darier disease.[10-13]

Appropriate laser parameters depend on the type of Er:YAG laser system used and the specific resurfacing indication. There is no consensus regarding the optimal laser parameters to use in every clinical setting. Laser surgeons commonly rely on their own experience to determine the most appropriate laser parameters to use in each case.

In this study, we apply the principles of laser-tissue interaction to develop a systematic understanding of the thermal and ablative effects of Variable Square Pulse (VSP) Er:YAG lasers under many different clinical resurfacing parameter combinations. A theoretical, tissue micro-explosions computer (MEC) model is used that links laser and tissue parameters with the clinical end effects of ablation and residual heat deposition in both non-ablative and ablative regimes.

A novel experimental method for determining residual, thermally affected skin layers is presented. The method is based on thermal camera measurements of the skin surface temperature decay following irradiation by a laser pulse.

The predictions of the theoretical MEC model are compared with measurements of ablation and heat deposition. The MEC model is found to be in good agreement with experiment, and thus suitable for implementation in VSP Er:YAG laser systems as a software tool for automatic calculation of the expected ablation and thermal depths.

II. MATERIALS AND METHODS

a) General

Wavelength is a key factor in the suitability of any laser for ablative skin procedures. There are currently three medical laser technologies, (Er:YAG, Er:YSGG (or Er,Cr:YSGG) and CO_2), whose laser wavelengths operate in the same regions as the major absorption peaks for water (see Fig. 1). [1, 15] Since the skin consists of 70% water, these three laser types can be effectively used for skin tissue ablation treatments.

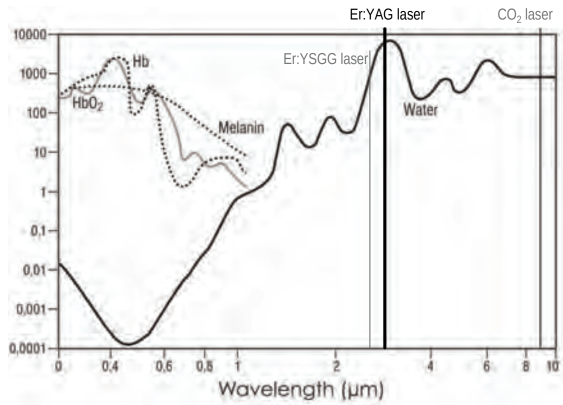

Fig. 1: The Er:YAG (2.9 µm) laser has the highest absorption in water and consequently in human skin. The Er:YSGG (2.7 µm) wavelength is located slightly below the water absorption peak, and absorbs only 3 times as well. An alternative laser that emits in the high absorption region is the CO2 laser (9.6 µm), however this laser is absorbed at 1/10 the absorption of Er:YAG in water, and is thus least suitable for laser resurfacing.

There are three steps in tissue heating upon laser irradiation. [16] The tissue is first heated directly within the optical absorption depth (*direct heating*) (Fig. 2).

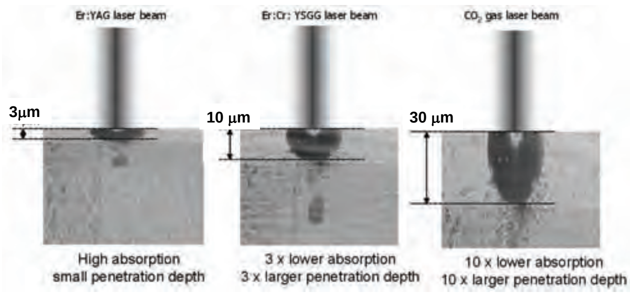

Fig. 2: The optical penetration depths in skin for the three ablative laser types. Depending on the laser type, different volumes of the illuminated tissue are directly heated by the laser light.

Closer study of the absorption peaks associated with Erbium lasers shows a 300% difference between the absorption coefficients in human skin of Er,Cr:YSGG (100 mm^{-1}) and Er:YAG (300 mm^{-1}). Similarly, the absorption coefficient, µ of the CO_2 laser is approximately 1000% smaller compared to that of the Er:YAG laser. As shown in Fig. 2, the Er:YAG laser wavelength thus penetrates approximately $1/\mu$ = 3 µm in the skin, while the Er:YSGG laser and CO_2 laser wavelengths respectively penetrate 10 µm and 30 µm into the skin.

Direct heating is followed by thermal diffusion that indirectly heats the deeper lying tissues (*indirect heating*) (Fig. 3). For shorter pulses, the time span for thermal diffusion is short, and the heat energy does not reach very deep into the tissue. For longer pulses, the heat has sufficient time to spread deeper into the tissue.

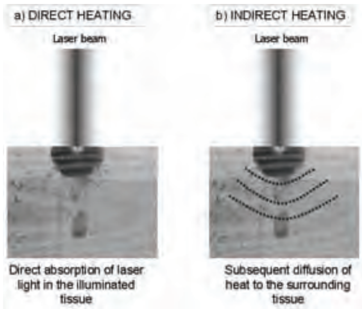

Fig. 3: Direct and indirect heating upon laser irradiation. The tissue is first heated directly within the optical absorption depth. This is followed by thermal diffusion that indirectly heats deeper lying tissue. The directly heated optical absorption depth layer is the smallest achievable thermal layer in the skin.

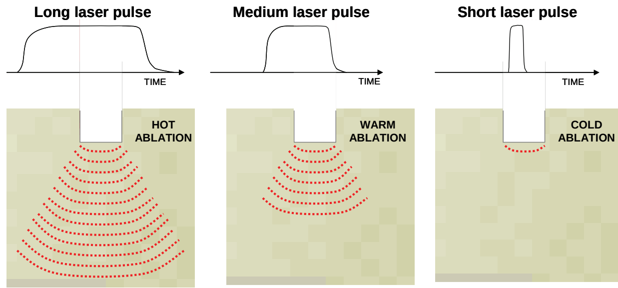

Fig. 4: Influence of laser pulse duration on heat dynamics. At longer pulse durations, heat has sufficient time to spread into the tissue. This results in deeper thermally modified skin tissue layers.

In the third step, the hottest part of the tissue close to the surface is evaporated, in effect reducing the depth of the thermally affected skin layer.

The difference in absorption properties of different types of lasers influences the volume of tissue directly heated to ablative temperatures, before the energy is diffused into the surrounding tissue. The optical penetration depth thus determines the smallest possible depth of thermally modified skin. While the thermal depth can be increased through indirect heating (Fig. 3), it cannot be reduced below the optical penetration depth (Fig. 2). Here, the Er:YAG laser is at an advantage as it allows the largest range of thermal depth control, and therefore the most complete range of treatments. By adjusting laser parameters, the Er:YAG laser can be used to perform "Er:YAG" type, as well as "Er:YSGG" and "CO_2" type laser treatments. Similarly, the Er:YSGG laser can be made to emulate the effects of the CO_2 laser, while the CO_2 laser is limited to the "CO_2" type treatments alone.

A key factor that determines the indirect heating depth, and therefore the laser treatment regime, is the laser pulse width. If the energy is delivered to the target in a very short time, ablation occurs before significant heat diffusion can take place. This results in less heat being distributed to the surrounding tissue. On the other hand, a long pulse width will allow more heat transfer before ablation takes place resulting in a greater thermal effect on the surrounding tissue (Fig. 4).

As an example, Figure 5 shows the thermal depth d_T at which the skin is indirectly heated to above 65^0 C, when laser fluences close to the ablation threshold are used (i.e. in a hot ablation regime). The thermal depth was calculated from the characteristic diffusion depth $x_d = (4D\ t_p)^{1/2}$, in which t_p is the laser pulsewidth, and the diffusion constant D for the skin is taken to be 1,1 x 10^{-7} m^2/s [15].

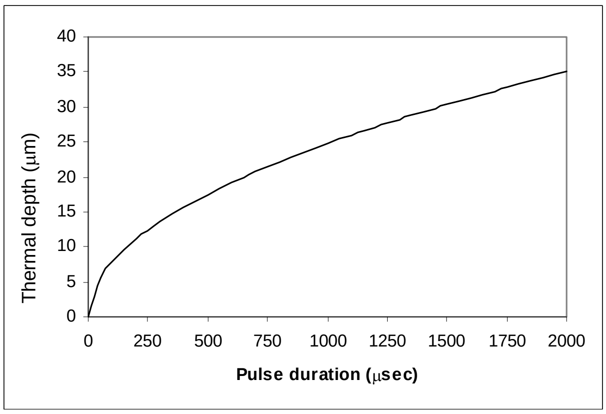

Fig. 5: The dependence of the thermally modified skin depth on the laser pulse width.

As can be concluded from Fig. 5, the laser light's ablative energy must be delivered to the skin in a temporal pulse of appropriate duration to control skin heating and ensure the efficacy, efficiency and safety of treatments. In the case of a long laser pulse or continuous irradiation, the heat that is generated by the laser light has sufficient time to diffuse deeper into the tissue from the irradiated surface area. This results in higher thermal effects inside the skin.

b) Measurements of VSP Er:YAG Laser Thermal and Ablation Depths

There have been numerous studies in which investigators have simulated the temperature rise in tissues, or used thermal cameras and thermocouples to measure temperature increase during laser irradiation.

[17-22] However, there are only a few studies of the residual heat following each ablative laser pulse. Radiological measurements of temperatures during and immediately following the laser pulse, in particular, are obscured by the high temperatures of the re-irradiated ejected tissue and plasma formation, limiting the accuracy of the method to predominantly sub-ablative regimes. In one of the studies, the residual heat deposition was determined by measuring the ratio of temperature rise on the backside of bovine block "calorimeters" induced by ablative and non-ablative laser pulses. [22]

In this study, the residual heat is determined directly by observing the characteristics of the temporal development of the surface temperature following pulsed laser irradiation, after the ablation plume has already decayed.[23-24]This method is particularly suited for studying residual heat in the ablative regime.

The skin surface temperature decay depends on the thickness of the heated tissue, and therefore on the deposited heat during the pulse. The thicker the heated layer, the longer the skin surface temperature rise will persist in time. The amount of heat that remains in the tissue after each laser pulse can be determined indirectly from the measured rate of the skin surface temperature decay (Fig. 6).

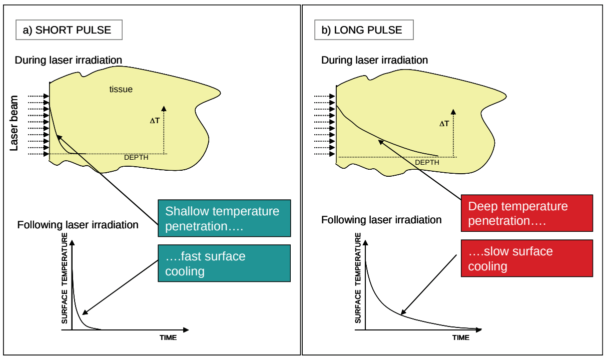

Fig. 6: Influence of pulse duration on the thickness of the heated layer at the end of a pulse, and on the subsequent skin surface cooling dynamics.

It can be assumed that the tissue surface temperature at the end of each pulse is always at the same approximate tissue-explosion temperature. The surface temperature decay following each pulse, depends on the thickness of the heated tissue, and therefore on the deposited heat during the pulse. The amount of heat that remains in the tissue after each laser pulse can thus be determined from the measured rate of the surface temperature decay.

A thermal camera (Flir ThermaCAM P45) was used to measure the skin surface temperature. Human skin obtained during abdominal surgery was used in the experiments. The camera was fixed in position above the skin surface and focused on the ablation site (Fig. 7). Since the imager software assumes a uniform body temperature the measured temperatures represent a weighted average of the skin temperature within the penetration depth of the detected thermal radiation (λ = 8-10 μm).

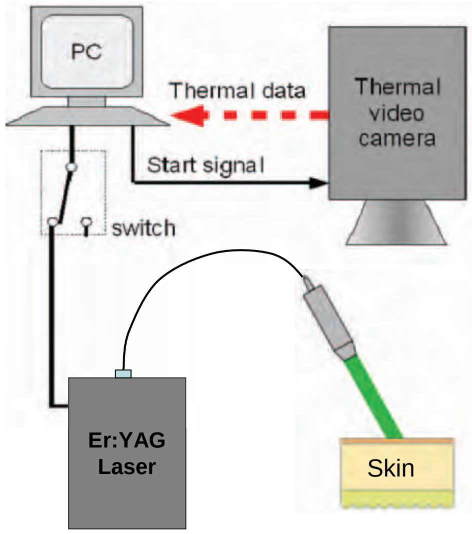

Fig. 7: Experimental set-up for thermal measurements.

The Er:YAG laser (XS Dynamis, Fotona) used in the study (Fig. 8) was fitted with a R11 non-contact handpiece with spotsizes from 2 to 10 mm.

Fig. 8: The Er:YAG laser (Fotona XS Dynamis) used in the experiment. [25]

The thermal camera was able to capture 50 images per second (one image every 20 ms) in quarter VGA resolution of 320x240 pixels. The image exposure time was approximately 5 milliseconds. The delay between the camera rate and the laser pulses was adjusted so that the maximum measured temperature would fall within the first measurement image following a laser pulse. By doing so the first measurement images were taken approximately 5 ms following a laser pulse. No alteration to the commercial laser device was made. The laser was fired as in a normal operation by pressing the footswitch, and the camera image was recorded following an emitted laser pulse. In each measurement, single laser pulses were delivered to different areas on the skin to avoid cumulative tissue desiccation. Sufficient time was taken between measurements in order to allow the skin to cool down to ambient temperature prior to each recording. The energy of the laser pulses was measured with an energymeter (Ophir Smarthead) at the R11 handpiece output.

The temperature distribution within the skin was calculated from the temporal decay of the skin surface temperature using a model that is described below.

The amount of heat that is deposited by a laser pulse decreases with distance within the tissue. This is partially due to the exponential decrease of laser light intensity within tissue, as provided by

$$I = I_0 \exp(-\mu x) \quad , \tag{1}$$

where I_0 is the incident laser intensity and μ is the optical absorption coefficient of the tissue for the particular incident laser wavelength.

The heat distribution within the tissue is additionally effected by the conduction of heat, i.e. heat diffusion into the surrounding tissue. In the limit of a negligible optical absorption depth, the thermal distribution which results from the uniform illumination of the surface, is approximated by the Gaussian function [26, 27]:

$$\Delta T = K \exp(-x^2/4Dt) \,, \tag{2}$$

where t is the duration of illumination, D is the thermal diffusivity of the tissue, and K is a constant that depends on the laser and tissue parameters. The longer the pulse duration and larger the thermal tissue diffusivity, the deeper the heat will spread away from the surface.

Ablation starts when the surface tissue is heated to the ablation temperature T_a. After that, and assuming a confined boiling model of laser ablation, [28] surface temperature stops increasing and remains fixed at the "boiling" temperature T_a throughout the ablation process. However, the temperature distribution away from the surface continues to change during the laser pulse because the diffusion does not stop after the ablation threshold has been reached.

In what follows, we assume that the diffusion penetration depth, $d = \sqrt{4Dt}$, is larger than the optical penetration depth, $1/\mu$, and that the thermal distribution at the end of an ablative pulse can be approximated by:

$$\Delta T = (T_a - T_0)\exp(-x^2/d_R^2) \tag{3}$$

Here the residual depth, d_R, represents the final depth of the heated layer, exactly at the end of a laser pulse and represents a measure of the residual heat deposition. The thinner the layer, the smaller the amount of the deposited residual heat Q_{res} will be:

$$Q_{res} = A\varrho c_p \int_0^{\infty} (T_a - T_0) \exp(-x^2/d_R^2)\, dx, \tag{4}$$

where A is the laser spot area, ϱ the tissue density, and c_p the tissue heat capacity.

Heat continues to diffuse into the tissue and surface temperature starts decreasing below T_a, after the laser pulse has ended. Here, we ignore the much slower convective surface cooling into the surrounding air.

Assuming a thermal distribution at the end of a laser pulse to be as described in (3), the temporal surface temperature evolution, T, following a laser pulse can be calculated using a one dimensional diffusion equation [26, 27]:

$$\frac{\rho c}{\lambda}\frac{\partial T}{\partial t} = \frac{\partial^2 T}{\partial x^2} \quad . \tag{5}$$

The one dimensional diffusion equation is taken to be a good approximation since the laser spot diameter is much larger than the diffusion depth. Alternatively, the initial T_a and d_R can be determined from the measured surface temperature decay by fitting the calculated temperature decay curves to the measured results.

The parameters as shown in Table 1 were used in the diffusion model.[28]

Table 1: Parameters used in the diffusion model.

Property	Value
ϱ [kg/m^3]	1100
λ [W/mK]	0.42
c_p [J/kgK]	1700
$D = \lambda/\varrho c_p$ [m^2/s]	$2.24 \cdot 10^{-7}$

For measuring ablation depths we used the recently introduced laser triangulation method that allows a fast and accurate determination of ablated volumes and depths. [29-31]

c) Theoretical Micro-Explosions Model

Most researchers agree that the erbium lasers' high ablation efficiency results from micro-explosions of overheated tissue water.[32,33] Such thermo-mechanical ablation mechanism has to be distinguished from mechanisms involving strong acoustic transients, plasma formation, or transient bubble formation, which can be encountered at higher laser intensities. Here, we apply a previously developed microscopic physical model of the micro-explosions. [28] The previously published model examined only the initiation of explosive material removal. In this paper, we improve upon this model by considering the ablation process above the ablation threshold. In the model, the process of confined boiling is modeled by considering the thermodynamic behavior of tissue water when it is heated within an elastic tissue.[28] The thermodynamic behavior of tissue water, which is the major absorber of Er:YAG (2.94 mm) laser irradiation, is combined with the elastic response of the surrounding solid medium. This is complemented by one-dimensional treatment of heat diffusion using a finite-difference scheme, and modeling protein denaturation kinetics with the Arrhenius integral. [34] The developed model explicitly links laser and tissue parameters with the end effects of ablation and residual heat deposition. We used this model to determine the influence of laser parameters on the desired surgical end effects in the treated tissue.

III. RESULTS

a) Ablation Depth

The fluence (F) is one of the main settings for skin resurfacing. It is defined as energy density:

$$F = E/A \qquad (6)$$

Where E is the energy of the laser pulse, $A = \pi s^2/4$ is the spot size area, and s is the spotsize of the laser beam at the skin surface. Usually it is calculated in J/cm^2. Typical Er: YAG fluences for skin resurfacing are between 0.5 to 50 J/cm^2 . [7, 8, 16]

Figure 9 shows the ablation depths, as calculated using the MEC micro-explosions computer model, for different pulse durations, as a function of laser fluence.

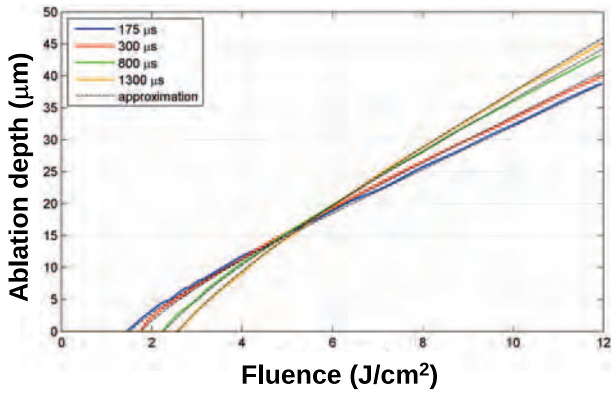

Fig. 9: Dependence of ablation depth on laser pulse fluence and pulse duration, as calculated from the MEC micro-explosions computer model.

The above calculated results are in a very good agreement with the measured ablation depths (Fig. 10).

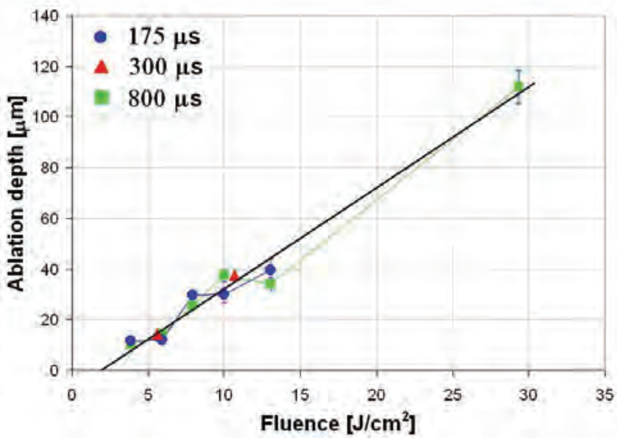

Fig. 10: Experimentally measured dependence of ablation depth on laser pulse fluence and pulse duration.

The MEC model and the experiment show that there is a threshold fluence under which there is no ablation (non-ablative regime). Ablation threshold fluence depends slightly on the pulse duration (it is higher for longer pulse durations), and ranges from 1.6 to 2.2 J/cm^2. Note that clinically a slight ablation may be observed already at lower fluences. This is attributed to skin surface inhomogeneities and surface sweat that facilitate earlier ablation.

Above the ablation threshold, the ablation depth grows approximately linearly with the fluence. Note that the dependence of the ablation depth on the pulse duration is relatively weak. The major parameter is the laser pulse fluence. Note also, that the exact values of the ablation threshold and of the linear ablation slope depend on the patient skin type, treatment location, skin hydration level and pulse duration.

b) Thermal Depth

Figure 11 shows measured temporal evolution of the skin surface temperature following Er:YAG laser pulses of different pulse duration modes in the hot ablation regime.

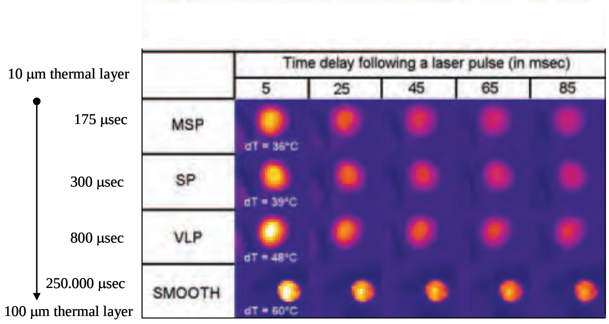

Fig. 11: Typical thermal images of the irradiated skin at 5, 25, 45, 65 and 85 msec following an Er:YAG laser pulse of 2J/cm². The temperature difference, ΔT, shown for different pulse duration modes, represents the temperature increase above the initial average room temperature within a central 1mm illuminated spot area.

After a pulse has ended, the temperature starts to decrease from the "boiling" temperature reached during the pulse. As expected, the observed thermal decay in Fig. 11 is fastest at the shortest, 175 µs (MSP) pulse where the heated skin layer is most shallow, and the slowest at the longest, 250.000 µs (250 ms; SMOOTH) pulse where the heated layer is thickest.

The influence of pulse duration can be clearly seen also by observing the skin temperatures at 5 ms and 85 ms delays following a laser pulse (Fig. 12).

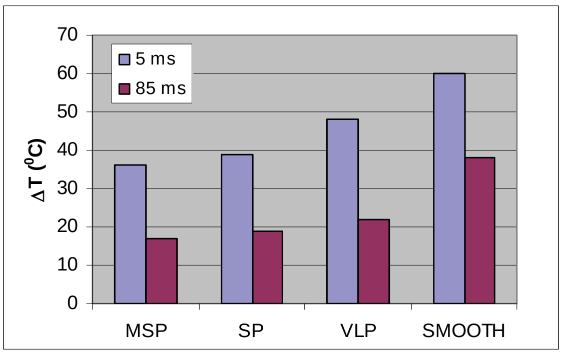

Fig. 12: Skin surface temperatures difference, ΔT, for different pulse durations modes at a 5 and 85 ms delay following a 2J/cm² laser pulse.

After 5 ms, the temperature difference, ΔT, drops to 36 ⁰C (0.175 ms, MSP mode), 39 ⁰C (0.3 ms, SP mode), 48 ⁰C (0.8 ms, VLP mode) and to 60 ⁰C (250 ms, SMOOTH mode). Similarly, at the 85 ms delay, the temperature increase, ΔT, drops to 17 ⁰C (MSP mode), 19 ⁰C (SP mode), 22 ⁰C (VLP mode) and to 38 ⁰C (SMOOTH mode).

As expected, the temperature increase, ΔT, depends strongly on the delivered laser pulse fluence. Figure 13 shows the skin surface temperature at a 25 ms delay as a function of laser pulse fluence.

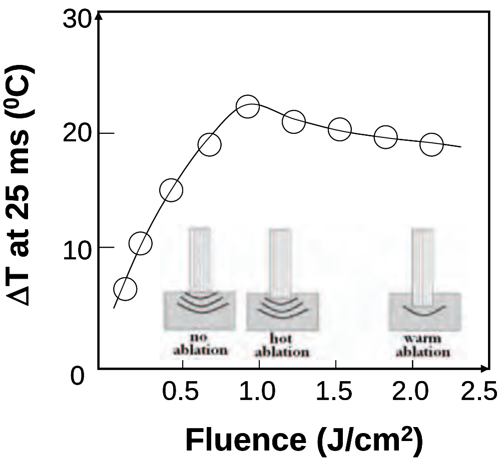

Fig. 13: Skin surface temperature 25 ms after an MSP mode laser pulse, as a function of laser pulse fluence.

Initially, the temperature increases with the fluence. At fluences below the ablation threshold there is NO ABLATION (see Fig. 14) and all the energy is released as heat, irrespective of the laser fluence. Above the ablation threshold, the ablation starts, while the remaining heated tissue layer remains thick (HOT ABLATION). At intermediate fluences the thermally effected layer becomes smaller (WARM ABLATION). At even higher fluences (not shown in Fig. 13), the ablation speed is higher than the rate at which heat diffuses into the tissue. All laser energy is thus used up for COLD ABLATION. The thermally affected tissue layer is confined to the directly heated tissue volume within the optical penetration depth.

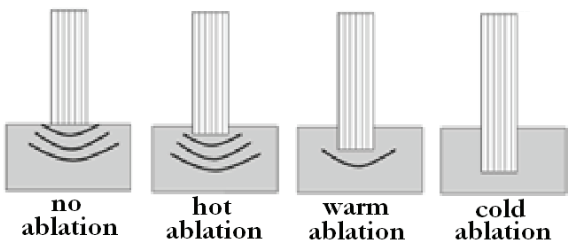

Fig. 14: In laser ablation we generally talk about one non-ablative and three ablative treatment regimes

Figure 15 shows the residual heat depth, d_R, for the MSP (175 μs) and VLP (800 μs) pulse duration mode, as obtained from experimentally measured skin surface temperature decays.

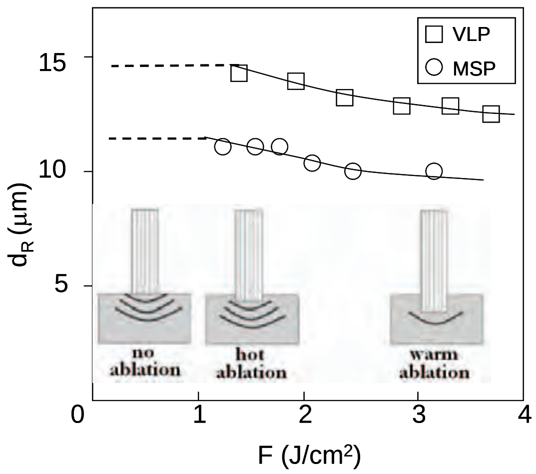

Fig. 15: Residual depth, d_R, of the thermal layer within the skin, as obtained from the thermal decay measurements for the VLP (800 μs) and MSP (175 μs) laser pulse durations.

Similarly, Fig. 16 shows the residual depth, d_R, for the MSP (175 μs) pulse duration mode, as calculated from the MEC micro-explosions numerical model.

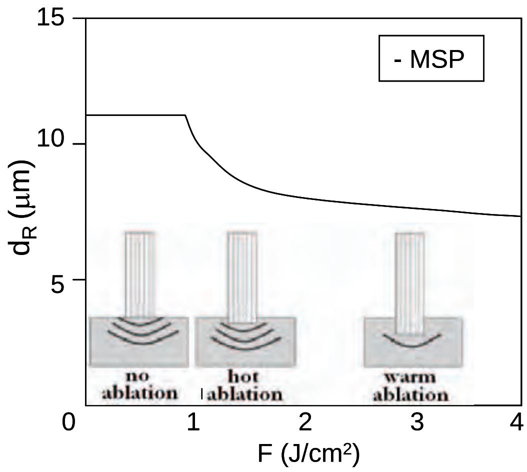

Fig. 16: Residual depth, d_R in skin for the MSP (175 μs) pulse duration mode, as obtained from the micro-explosions model.

The experiment and the theoretical MEC model are in good agreement, confirming the accuracy of the model. Both, measurements and the micro-explosion model show that the depth of the residual heated skin layer starts to decrease for fluences above the ablation threshold. The residual depth is also observed to be larger for longer pulse durations (see also Fig. 4).

Clinically, the more relevant information is the depth of the thermally modified skin tissue layer (thermal depth, d_T). We modeled the protein denaturation process at each point in space and time by calculating the damage parameter Ω according to the Arrhenius equation of protein denaturation kinetics:

$$\Omega\,(z,t) = A \int_0^t \exp\,(-E/RT(z,t'))\,dt'\,, \qquad (7)$$

with parameter values $A=3.1\times10^{98}$ s^{-1} and $E = 6.28 \times 10^8$ J/kmol.[27, 28] The parameter z measures the distance of a point from the skin surface. Tissue is assumed to be irreversibly modified when Ω exceeds 0.5. Figure 17 shows the calculated depth of the thermally modified layer, d_T, as a function of laser fluence for the MSP pulse duration mode.

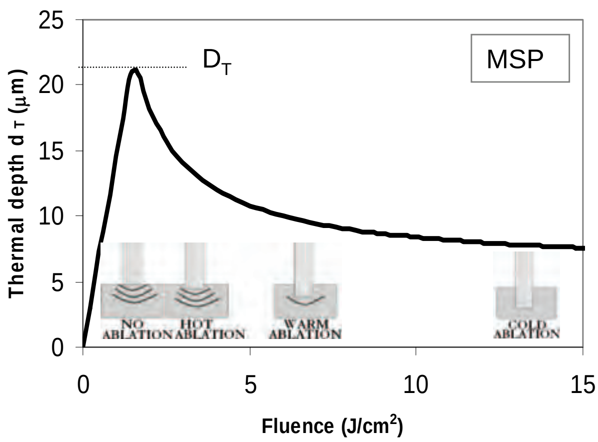

Fig. 17: Depth of thermally modified layer, d_T, as a function of laser fluence for MSP (175 μs) pulse duration mode.

In the non-ablative region, the thermal depth d_T increases with fluence up to the maximum thermal depth, D_T, when the ablation threshold is reached. The thermal depth then starts to decrease towards higher fluences: from hot to warm, and finally to the cold ablation regime. Similar dependences apply for all VSP Er:YAG pulse mode durations.

IV. DISCUSSION

a) Nine Treatment Regimes

As shown above, the thermal and ablation depths of VSP Er:YAG lasers depend on the combination of two parameters; pulsewidth and fluence. The VSP technology-supported Er:YAG laser is an extremely versatile and precise skin resurfacing tool. The control of pulsewidth and laser fluences provides a wide range of treatment options that can be depicted as a simple matrix (see Fig. 18). [16]

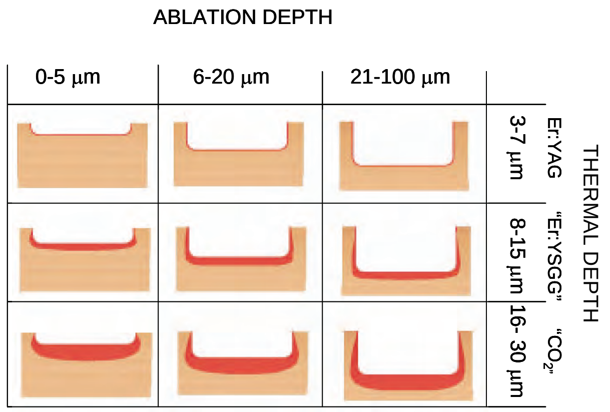

Fig. 18: Approximate ablative and thermal depths for the nine VSP treatment regimes. [16]

VSP Er:YAG laser treatment regimes are thus defined as follows (Table 2):
a) **Cold regime** with thermal depths of approximately 3-7 µm;
b) **Warm regime** with thermal depths of approximately 8-15 µm;
c) **Hot regime** with thermal depths above approximately 15 µm.

Table 2: Three VSP Er:YAG laser thermal treatment regimes. [16]

Er:YAG Thermal Regime	Thermal Depth (µm)
COLD	3 – 7
WARM	5 – 15
HOT	above 15

Note that the VSP Er:YAG cold, warm and hot regimes correspond approximately with the thermal depth limits of the Er:YAG (cold), Er:YSGG (warm) and CO_2 (hot) lasers. By selecting VSP Er:YAG laser regimes, the practitioner tunes the laser effect from a purely "Er:YAG type" laser treatment, to an "Er:YSGG type" laser treatment, and at the longest pulsewidths to a "CO_2 type" laser treatment.

There are also three VSP Er:YAG laser treatment regimes (*Light*, *Medium*, and *Deep*) in terms of their ablative depth (see Table 3):

Table 3: Three Er:YAG ablation regimes in terms of ablation depth. [16]

Er:YAG Ablative Regime	Ablation Depth (µm)
LIGHT	0 – 5
MEDIUM	6 – 20
DEEP	above 20

The combination of Er:YAG thermal treatment regimes with the treatment regimes based on ablation depth provides a matrix of nine VSP treatment regime options, as shown in Figure 18, together with the corresponding ablative thermal depths. The recommended treatment parameters for the nine regimes are shown in Figure 19.

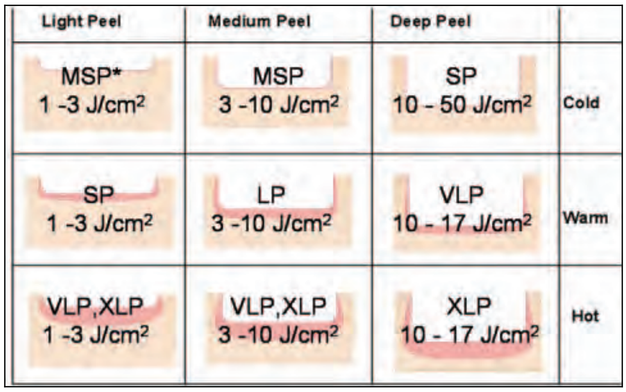

Fig. 19: Recommended treatment parameters for the nine VSP Er:YAG treatment regimes. [16]

Note that the recommended values are only approximated, as the exact values depend on skin type, treatment location, skin hydration levels and other parameters. The ablation threshold fluence can thus vary in real patient situations. Also note that the indicated boundaries between the regions of cold, warm and hot ablation are only approximate. In reality more gradual transitions exist between these treatment regimes.

The correct therapeutic ablation depth is the minimum depth needed to achieve the desired clinical result, whether it is for the effacement of rhytids, removal of photo-damage and/or collagen tightening. Generally, laser resurfacing is performed by treating the area completely, until the to-be-removed lesions have been ablated or until punctate bleeding appears, which indicates the papillary dermis has been reached. At the papillary dermis level a maximum therapeutic effect is achieved with a minimum risk of side effects. Continuing to treat deeper than the papillary dermis has minimal clinical benefits, while the potential of complications and side effects may even exponentially increase. With clinical experience it is advisable to select laser treatment settings that will give the desired result in 2-4 passes. Visual clinical end-points for the three ablative regimes are shown in Figures 20a to 20c.

Light Peel

Fig. 20a: Light Peel. Whitish coloring of the skin after administering laser pulses generally indicates the Er:YAG laser treatment has reached the intra-epidermal level. [16]

Medium Peel

Fig. 20b: Medium peel. Yellowish coloring of the skin after administering laser pulses generally indicates the Er:YAG laser treatment has reached the deep epidermal level. [16]

Deep Peel

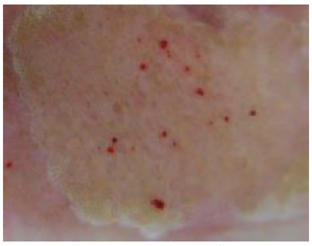

Fig. 20c: Deep peel. Punctate bleeding suggests that the papillary dermis has been reached. Generally this indicates that the clinical end-point has been reached in Er:YAG laser resurfacing treatments. [16]

As a general rule, the final treatment outcome is more pronounced when more aggressive treatment parameters are used. More aggressive treatments are achieved with deeper ablation and thermal parameters while patient downtime and risk of complications increase. An approximate relation of the nine treatment regimes with regards to the efficacy and downtime is shown in Figure 21. Clinically obtained downtimes for cold, warm and hot light peels are respectively 12-48 hours, 12-72 hours, and 4-5 days. The downtime for a *cold medium peel* (papillary dermis) is 7-10 days.

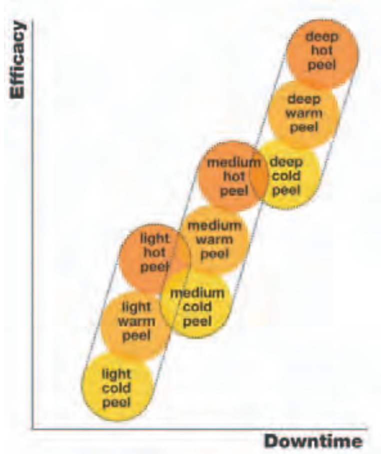

Fig. 21: Approximate relation of the nine VSP Er:YAG laser ablative treatment regimes with regard to the efficacy and downtime. [16]

Examples of full field ablative Er:YAG treatments are depicted in Figs. 22-24.

Before **After**

Fig. 22: Ablative skin lesion removal. Courtesy of R. Sult.

Before **40 days after**

Fig. 23: Perio-oral skin resurfacing. Courtesy of dr. G. Lupino.

Before **3 months after**

Fig. 24: Removal of Xanthelasma Palpebrarum. Courtesy of dr. Drnovsek.

b) Super Long SMOOTH and V-SMOOTH Modes

In addition to the nine basic VSP Er:YAG treatment regimes, there is also a unique additional tenth treatment regime; the non-ablative SMOOTH (t_p =20 ms), [35-48] and more recently variable, V-SMOOTH (t_p = 100-500 ms) mode.[34]

In the SMOOTH mode, [35] laser energy is transmitted as heat onto the skin surface, without any resulting ablation, and is then dissipated into the deeper tissue layers. If laser energy is delivered to the skin surface in a time period longer than the Thermal Relaxation Time (TRT) of the epidermis (estimated to be around between 10 and 100 msec depending on the thickness), the epidermis has sufficient time to cool by dissipating the heat into the deeper skin layers. Thus temperatures required for ablation are reached at much higher fluences. The TRT is the time required for the tissue temperature to decrease by approximately 63%. And if at the same time laser energy is delivered in a time period that is shorter than the combined skin TRT (estimated to be in the range of 500 msec) then the skin does not have time to cool off during the laser pulse. The delivered laser energy thus results in an overall build-up of heat and creates a temperature increase deep in the papillary dermis.

The above principle is employed when the super-long pulses of SMOOTH mode are used. SMOOTH and V-SMOOTH pulses deliver laser energy onto the skin in a fast sequence of low fluence laser pulses inside an overall variable length super-long pulse of 100-500 msec.

Because the super-long SMOOTH pulses are longer than the epidermal TRT, the threshold ablation fluence is much higher than 2 J/cm² and the conditions for ablation are more difficult to reach. The effect of SMOOTH mode is mainly thermal modification of the skin, without any significant ablation of the epidermis. The thermal depths d_T in the V-SMOOTH (t_p = 100 ms) mode as a function of laser fluence, are shown in Figure 26. For comparison, the thermal depths for the short, MSP (t_p = 0.175 ms) pulse are also shown.

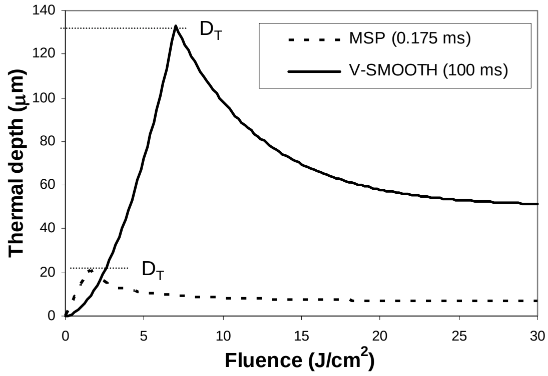

Fig. 26: Large thermal depths without skin ablation can be achieved with the Fotona V-SMOOTH mode.

Since in the super long SMOOTH mode the ablation threshold is high the maximal thermal depth, D_T, which is always reached at the threshold fluence is also high. Table 4 shows the maximal thermal depths, D_T, calculated using the MEC theoretical model for all currently available VSP Er:YAG pulse duration modes.

Table 4: The ablation threshold fluences, and the corresponding maximum thermal depths, for the currently available VSP Er:YAG pulse duration modes. V-SMOOTH mode pulses are generated in a slightly different manner than the SMOOTH mode pulses. For this reason, the ablation thresholds and thermal depths of the V-SMOOTH pulses follow a different dependency on pulse duration than the SMOOTH mode.

Pulse Duration Mode	Ablation Threshold (J/cm²)	Maximal Thermal Depth, D_T (μm)
MSP (0.175 ms)	1.6	21
SP (0.3 ms)	1.8	26
LP (0.6 ms)	2.0	32
VLP (0.8 ms)	2.2	37
XLP (1.3 ms)	2.6	45
SMOOTH (250 ms)	6.1	81
VSMOOTH (100 ms)	7.0	132
VSMOOTH (200 ms)	7.4	125
VSMOOTH (300 ms)	7.7	120
VSMOOTH (400 ms)	7.85	110
VSMOOTH (500 ms)	8.0	95

Histological investigations show that SMOOTH and V-SMOOTH mode treatments result in collagen thermal that extends deeper than 100 μm below the epidermal-dermal junction. [12, 36-40, 46] Clinically, this collagen thermal results in visible and long-lasting reduction of wrinkles and scars (see Fig. 27). [41-42]

Fig. 27: SMOOTH mode treatment of the flaccidity in arms. Courtesy of dr. C. Pidal.

c) Fractional Treatments

Fractional laser photothermolysis is the latest in the broad range of VSP Er:YAG laser techniques. [49-51] This technique promises a novel means of providing treatments that would be as effective as traditional Er:YAG approaches while further reducing their downtime and risk.[52-57] The fractional technique is based on a concept of producing an array of microscopic wounds on the skin surface that are rapidly reepithelialized by the surrounding, undamaged tissue, sparing the epidermis in the untreated areas (Fig. 28).

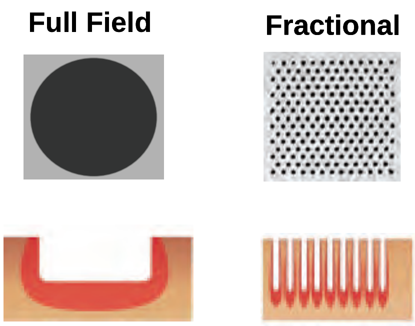

Fig. 28: As opposed to the traditional, full field resurfacing, the fractional resurfacing is based on a concept of producing an array of microscopic wounds.

With the fractional handpieces, the practitioner can perform all nine basic VSP ablative and SMOOTH treatments at fully clinically tested laser parameters (see Fig. 29). The only difference is that the skin is treated with pixelated Er:YAG laser beams (see Fig. 30).

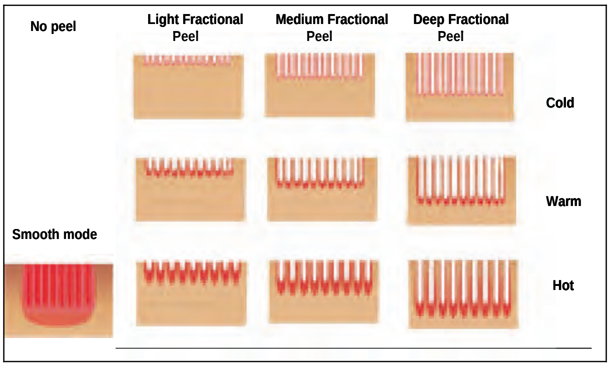

Fig. 29: The fractional treatment regimes are in principle the same as the basic VSP Er:YAG treatment regimes, but through pixelation they are less invasive and have shorter downtimes

Fig. 30: Fractional skin resurfacing.

There are two types of fractional handpiece technologies, stamping and scanning (Fig. 31).

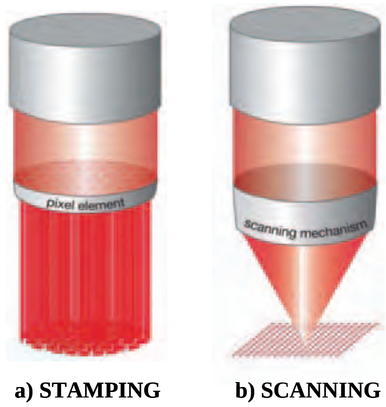

Fig. 31: Two types of fractional handpiece technologies.

With stamping fractional handpieces, the full laser beam (spot) is divided into many small beams (micro dots or pixels), and the pixel fluence is comparable to the total laser beam fluence. The pixel energy is a fractional part of the total pulse energy. A typical stamping fractional handpiece is shown in Fig. 32.

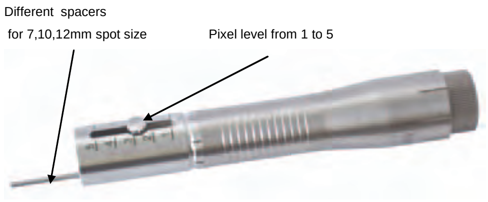

Fig. 32: Stamping fractional handpiece (PS01, Fotona d.d.). [25]

A typical stamping fractional beam profile is shown in Figure 33.

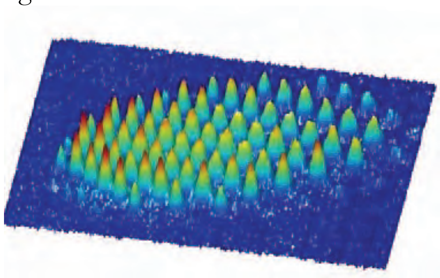

Fig. 33: A typical PS01 handpiece pixel beam profile. Note the soft laser intensity transition between the pixels.

With scanning fractional handpieces, the laser beam is concentrated and focused into a very small spot that is scanned over a treated area. The micro dot energy is the same as the full field pulse energy which enables higher fluences and deeper treatments. Also, the treatment areas and the dot density can be easily changed via the keyboard. A typical scanning fractional handpiece is shown in Fig. 34.

Fig. 34: A typical scanning fractional handpiece (F22 F-Runner, Fotona d.d.). [25]

Scanning fractional handpieces enable an additional, extremely deep ablative modality (above 100 μm). In addition, the scanning fractional handpieces allow more control and variation in the treated area pattern (Fig. 35).

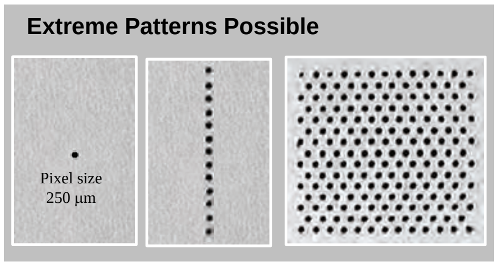

Fig. 35: A wide range of patterns is available with the scanning fractional handpieces (shown is an example of the F22 scanner patterns).

d) TURBO Mode

When very large ablation depths are desired, the ablation depth can be increased also by using the so-called TURBO mode.[58] This mode allows the practitioner to determine the treatment depth by selecting the fluence and the number of pulses to be stacked on the same treatment area (see Fig. 36). As always in ablative mode, the thermal depth is determined mainly by the pulsewidth.

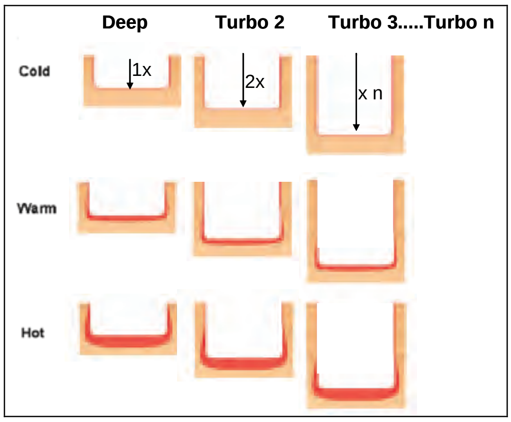

Fig. 36: The TURBO enhancement mode provides increased ablative action.

When, for example, a *cold deep peel* treatment regime is selected with the addition of the TURBO 3 modality, the ablative depth (but not the thermal depth) will be three times larger compared to the basic *cold deep peel* treatment regime.

Our measurements also show that when the TURBO mode is used in highly ablative fractional treatments, the contours of the micro-channels created by fractional ablation are more pronounced and sharper, if compared to equivalent energy single pulses (see Fig. 37).

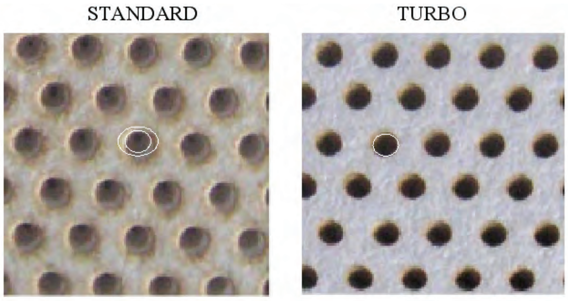

Fig. 37: TURBO mode produces sharper edges compared to a standard single giant laser pulse.

The images above clearly show the distinct differences in micro-channel contour sharpness between equivalent energy standard single pulses (left) and TURBO pulses (right). Both scans were conducted using the F-Runner scanner with equivalent settings

We attribute the difference in micro-channel sharpness to the scattering of high energy single pulses due to the formation and screening effect of tissue debris as illustrated in Fig. 38 below.

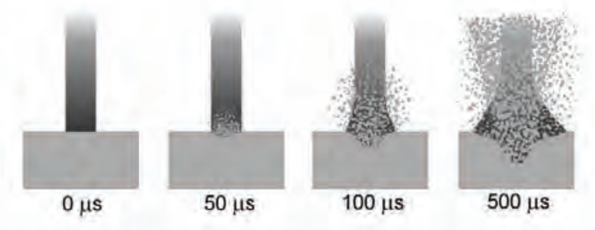

Fig. 38: The laser beam scattering effect is induced by ablated particles.

In single, high energy pulses the scattered laser beam irradiates the tissue surrounding the micro-channel. Although the scattered beam is sub-ablative, it will create thermal effects in the micro-channel surroundings, the therapeutic effects or benefits of which cannot be defined or controlled. The scattering effect and loss of sharp micro-channel contour definition become more pronounced with more aggressive ablation settings since the debris will be bigger.

By stacking, lower energy pulses in extremely short intervals in one TURBO pulse, the aforementioned ablation-limiting effects are avoided, and more defined and precise micro-channels are created.

The TURBO mode provides VSP Er:YAG laser fractional treatments greater flexibility. It allows fractional treatments to be accomplished from the keratinous layer to depths the practitioner deems necessary for the clinical application at hand. TURBO mode can be used to reach deeper into the dermis than traditional (non-fractional) resurfacing techniques (see Fig. 39).

Fig. 39: A histological picture of a deeply ablated pixel, using a TURBO mode (F-22, Fotona d.d.)

V. CONCLUSION

Dependences of skin ablation and thermal depths on VSP Er:YAG laser parameters were determined experimentally and theoretically. A micro-explosions computer (MEC) theoretical model was developed, that explicitly links laser and tissue parameters with the end effects of ablation and residual heat deposition. The predictions of the MEC model were found to be in a good agreement with the experiment.

Thermal depths, and to some degree also ablation depths, are a relatively complex function of the laser pulse width and pulse fluence. Nevertheless, the practitioner does not need to be preoccupied with these dependencies; the latest VSP Er:YAG laser systems already have a software solution implemented that is based on the MEC model.[59] The MEC software automatically calculates the expected ablation and thermal depths for the selected parameters and shows them on the laser system screen.

The advanced VSP Er:YAG technology thus enables the practitioner to easily adjust the laser treatment modality to the patient type and the treated indication. There is no other laser wavelength, nor technology that allows similar levels of treatment control and precision, while providing the extent of treatment modalities presented in this paper.

REFERENCES

1. Spoor TC, Moy RL (2001) Facial Rejuvenation, Martin Dunitz Ltd. , pp. 105-148.
2. Utley DS, Koch RJ, Egbert BM (1999) Histologic analysis of the thermal effect on epidermal and dermal structures following treatment with the superpulsed CO2 laser and the erbium: YAG laser: an in vivo study. Lasers Surg Med. 24(2):93-102.
3. Tanzi EL, Alster TS (2003) Single-pass carbon dioxide versus

multiple-pass Er:YAG laser skin resurfacing: a comparison of postoperative wound healing and side-effect rates. Dermatol Surg. 29(1):80-4
4. Cole RP, Widdowson D, Moore JC (2008) Outcome of erbium:yttrium aluminium garnet laser resurfacing treatments. Lasers Med Sci. 23(4):427-33.
5. Kunzi-Rapp K, Dierickx CD, Cambier B, Drosner M (2006) Minimally invasive skin rejuvenation with erbium: YAG laser used in thermal mode, Lasers Surg Med. 38:899-907
6. Variable Square Pulse (VSP) is a Fotona d.d. (www.fotona.com) proprietary technology for the generation and control of laser pulses.
7. M. Lukac, T. Sult, R. Sult (2007) New Options and Treatment Strategies with the VSP Er:YAG Aesthetic Lasers, J. Laser and Health Academy, Vol. 2007, No.1. www.laserandhealth.com
8. M. Lukac (2007) New Options and Tretment Strategies with VSP Er:YAG Aesthetic Lasers, J. Cosmetic Laser Therapy.
9. Pozner JN, Roberts TL 3rd (2000) Variable-pulse width ER:YAG laser resurfacing. Clin Plast Surg. 27(2):263-71,
10. Alster TS, Lupton JR (2001) Erbium:YAG cutaneous laser resurfacing. Dermatol Clin. 19(3):453-66.
11. Teikemeier G, Goldberg DJ (1997) Skin resurfacing with the erbium:YAG laser. Dermatol Surg. 23(8):685-7.
12. Pozner JN, Goldberg DJ (2006) Superficial erbium:YAG laser resurfacing of photodamaged skin. J Cosmet Laser Ther. 8(2):89-91.
13. Kaufmann R (2001) Role of Erbium:YAG laser in the treatment of aged skin. Clin Exp Dermatol. 26(7):631-6.
14. Scanner Optimized Efficacy (SOE) is a Fotona d.d. technology. www.fotona.com.
15. Anderson R, Parrish J (1981) The optics of human skin, J Invest Dermatol. 88:13-19.
16. Lukac M , Vizintin Z, Kazic M, Sult T, Novel Fractional Treatments with VSP Erbium YAG Aesthetic Lasers, J. Laser and Health Academy, Vol. 2008, No.1. www.laserandhealth.com
17. Zuerlin MJ, Fried D, Seka W, Featherstone JDB (1989), Modelling thermal emission in dental enamel induced by 9-11 μm laser light, Appl. Surf. Science 127-129 863-868.
18. Armengol V, Jean A, Marion D (2000) Temperature rise during Er:YAG and Nd:YAP laser ablation of dentin, J Endod, 26: 138-141
19. Fried D, Visuri SR, Featherstone JDB, Walsh JT, Seka W, Glena RE, McCormack SM, Wigdor HA (1996) Infrared radiometry of dental enamel during Er:YAG and Er:YSGG laser irradiation, J. Biomedocal Opt. 1(4) 455-465
20. Venugopalan V, Nishioka NS, Mikic BB (1996) Thermodynamic response of soft biological tissues to pulsed infrared laser irradiation, Biophysical J., 70: 2981-2993.
21. Harris DB, Fried D, Reinisch L, Bell T, Schachter D, From L, Burkart J (1999) Eyelid resurfacing, Lasers Surg Med. 25:107-122
22. Fried D, Ragadio J, Champion A (2001) Residual heat deposition in dental enamel during IR laser ablation at 2.79, 2.94, 9.6, and 10.6 μm, Lasers Surg Med. 29: 221-229
23. Perhavec T, Diaci J (2009) Comparison of Heat Deposition of Er:YAG and Er,Cr:YSGG Lasers in Hard Dental Tissues, J. Laser and Health Academy, Vol. 2009, No.1. www.laserandhealth.com.
24. Perhavec T, Lukac M, Diaci J, Marincek M (2009) Heat deposition of erbium lasers in hard dental tissues. J. oral laser appl., 2009, vol. 9, no. 4, pp. 205-212.
25. See: www.fotona.com.
26. Cox (2007), Introduction to Laser-Tissue Interactions, PHAS 4886 Optics in Medicine, October 2007, 1-61.
27. Niemz MH (2002) Laser-Tissue Interactions: Fundamentals and Applications, 2nd edition, Springer, pp. 58-85.
28. Majaron B, Plestenjak P, Lukac M (1999) Thermo-mechanical laser ablation of soft tissue: modeling the micro-explosions, Appl.Phys.B 69:71-80.
29. Perhavec T, JDiaci J (2008). Comparison of Er :YAG and Er,Cr :YSGG dental lasers, J. Oral Laser Appl., 8 :87-94.
30. Perhavec T, Gorkic A, Bracun D, Diaci J (2009) A method for rapid measurement of laser ablation rate of hard dental tissue. Optics and Laser Technology 41(4): 397-402
31. Diaci J (2008) Laser Profilometry for the Characterization of Craters Produced in Hard Dental Tissues by Er:YAG and Er,Cr:YSGG Lasers, Journal of the Laser and Health Academy, vol. 2008, 2.
32. Vogel A, Vengugopalan V (2003) Mechanisms of Pulsed Laser Ablation of Biological Tissues, Chem.Rev. 103: 577-644.
33. Majaron B, Sustersic D, Lukac M, Skaleric U, Funduk N (1998) Heat diffusion and debris screening in Er:YAG laser ablation of hard biological tissues, Appl.Phys.B, 66: 1-9
34. V-SMOOTH is a variable pulse length Er:YAG pulse sequence available in VSP Er:YAG S-Runner scanner handpieces developed by Fotona d.d. www.fotona.com.
35. SMOOTH is a super long Er:YAG pulse sequence available in VSP Er:YAG lasers developed by Fotona d.d..
36. Beltram M, Drnovsek-Olup B (2005) New collagen synthesis in skin fibroblasts after Er:YAG laser skin resurfacing. Lasers Surg med. suppl. 17, pp. 33.
37. Beltram M, Drnovsek-Olup B (2008) Quantitative analysis of new collagen synthesis after Er:YAG laser skin resurfacing with biomolecular technicque. Lasers Surg Med., 2008, suppl. 20, pp. 35.
38. Drnovsek-Olup B, Beltram M (2002) ER:YAG dual-mode skin resurfacing long-term follow-up. Lasers Surg. Med. (Online), pp. 1-9.
39. Beltram M, Drnovsek-Olup B (2003) In situ hybridization analysis of type 1 collagen gene expression after Er:YAG laser skin resurfacing. Lasers Surg. Med., Suppl., , suppl. 15, pp. 8.
40. Drnovsek-Olup B, Beltram M, Pizem J (2004) Repetitive Er:YAG laser irradiation of human skin : a histological evaluation. Lasers Surg Med., 2004, letn. 35, št. 2, pp. 146-151.
41. Drnovsek-Olup B, Beltram M (2002) Long term evaluation of periocular Er:Yag laser skin resurfacing combined with blepharoplasty. V: ESOPRS Meeting. Abstracts. [Münster: Universitäte-Hauptgebäude, 2002].
42. B. Drnovsek-Olup, M. Beltram (2002) Er:Yag laser skin resurfacing long term follow-up. Lasers surg. med. Suppl. 14: 66-67.
43. Drnovsek-Olup B, Beltram M. Collagen synthesis after laser skin resurfacing : in situ hybridization of pro alpha 1 collagen type 1. V: ESOPRS Gothenburg 2003 : [abstracts].
44. Beltram M, Drnovsek-Olup B (2004). Histological and biomolecular analysis of new collagen synthesis after Er:YAG laser skin resurfacing. V: Alpe Adria community ophthalmology 2004 : [program & abstracts book], October 8th to 10th, 2004. Munich: University of Technology, 2004, pp. 73.
45. Beltram M, Drnovsek-Olup B (2004) Histological and biomolecular analysis of new collagen synthesis after "smooth" mode Er:Yag laser skin. Lasers surg. med., Suppl. 16: 56.
46. Drnovsek-Olup B, Beltram M (2005) Histological comparison between different modes of Er:YAG laser skin resurfacing-ablative, dual mode and smooth mode resurfacing. Lasers Surg Med. suppl. 17:9.
47. Drnovsek Olup B, Vedlin B (1997) Use of Er:YAG laser for benign skin disorders. Lasers Surg Med. 21:13-19
48. Majaron B, Srinivas SM, Huang HL, Nelson JS (2000) Deep coagulation of dermal collagen with repetitive Er:YAG laser irradiation, Lasers Surg Med. 26: 215-222
49. Dierickx CC et al. (2008) Micro-Fractional Ablative Skin

Resurfacing with Two Novel Erbium Laser Systems, Lasers Surg Med. 40:113-123
50. Pozner JN, Glanz S, Goldberg DJ (2007) Fractional erbium resurfacing: Histologic and early clinical experience. Lasers Surg Med. 39:S19:73
51. Lapidoth M, Odo MEY, Odo LM (2008) Novel Use of Erbium (2,940nm) Laser for Fractional Ablative Photothermolysis in the Treatment of Photodamaged Facial Skin: A Pilot Study, Dermatology Surgery, 34:2-6.
52. Volovec L (2008) Skin Rejuvenation with Fractionated Ablative Er:YAG Laser, 7th Croatian Congress of Plastic, Reconstructive and Aesthetic Surgery, Book of abstracts, Split, Croatia 1-5 October, 2008.
53. Trelles MA, Velez M, Mordon S (2008) Correlation of Histological Findings of Single Session Er:YAG Skin Fractional Resurfacing With Various Passes and Energies and the Possible Clinical Implications, Lasers Surg and Med. 40:174-177
54. Vizintin Z (2008) Fractional Laser Technologies – Overview, 7th Croatian Congress of Plastic, Reconstructive and Aesthetic Surgery, Book of abstracts, Split, Croatia, 1-5 October, 2008.
55. Kozarev J (2008) Treatment of Stretch marks with fractional ablative Er:YAG laser, Belgrade, Serbia, June 2008
56. Pidal C (2008) Estria Roja con Fractional Smooth ErYAG laser, VIII Curso Internacional de Procedimientos Estéticos Minimamente Invasivos "Avances en Medicina Estética y Cirugía Minimamente Invasiva", Lima, Peru, 2008
57. Massoud K (2007) Fractional Laser Skin Resurfacing, International Aesthetic Laser Seminar, Dubai, October 2007.
58. TURBO is a Fotona d.d technology. www.fotona.com.
59. MEC software is available in Dynamis laser family developed by Fotona d.d.. www.fotona.com.